Simulation Study of a Gramicidin/Lipid Bilayer System in Excess Water and Lipid. I. Structure of the Molecular Complex

See-Wing Chiu,*# Shankar Subramaniam,*#§¶‖ and Eric Jakobsson*#§¶‖

*National Center for Supercomputing Applications, #Department of Molecular and Integrative Physiology, §Department of Biochemistry, ¶Center for Biophysics and Computational Biology, and ‖Beckman Center for Advanced Science and Technology, University of Illinois, Urbana, Illinois 61801 USA

ABSTRACT This paper reports on a simulation of a gramicidin channel inserted into a fluid phase DMPC bilayer with 100 lipid molecules. Two lipid molecules per leaflet were removed to insert the gramicidin, so the resulting preparation had 96 lipid molecules and 3209 water molecules. Constant surface tension boundary conditions were employed. Like previous simulations with a lower lipid/gramicidin ratio (Woolf, T. B., and B. Roux. 1996. *Proteins: Struct., Funct., Genet.* 24:92–114), it is found that tryptophan-water hydrogen bonds are more common than tryptophan-phospholipid hydrogen bonds. However, one of the tryptophan NH groups entered into an unusually long-lived hydrogen bonding pattern with two glycerol oxygens of one of the phospholipid molecules. Comparisons were made between the behavior of the lipids adjacent to the channel with those farther away. It was found that hydrocarbon chains of lipids adjacent to the channel had higher-order parameters than those farther away. The thickness of the lipid bilayer immediately adjacent to the channel was greater than it was farther away. In general, the lipids adjacent to the membrane had similar orientations to those seen by Woolf and Roux, while those farther away had similar orientations to those pertaining before the insertion of the gramicidin. A corollary to this observation is that the thickness of the hydrocarbon region adjacent to the gramicidin was much thicker than what other studies have identified as the "hydrophobic length" of the gramicidin channel.

INTRODUCTION

The gramicidin peptide forms the smallest known protein ion channel, a dimer consisting of two gramicidin molecules that contain 15 amino acids each. Because of its small size, the relative ease with which it partitions into membranes to form channels, and the relative ease of synthesis of native gramicidin and variants, gramicidin has long been a useful model system with which to study permeation through membrane proteins, principles of membrane protein structure, and protein-lipid interactions. Secreted by the bacterium *Bacillus brevis*, gramicidin was early identified as an antibiotic (Dubos and Hotchkiss, 1941). Single-channel ionic currents were observed in gramicidin before the invention of the patch clamp (Hladky and Haydon, 1970). In 1971, it was established by solution NMR techniques that the structural motif of the gramicidin membrane channel is a pair of β-bonded helices disposed head-to-head relative to each other (Urry, 1971). Subsequent solid-state NMR studies established that the helices are right-handed and provided a high-resolution structure (Ketchem et al., 1993), albeit one with some possible ambiguity about the dominant side-chain conformations (Koeppe et al., 1994). Interestingly, there is an alternative structural motif that provides a pore large enough to transport ions. This is a double coil, and is the form that crystallizes out of organic solvents (Langs, 1988; Wallace and Ravikumar, 1988). However, the head-to-head β-helical motif prevails in lipid bilayers. The preference for this motif is probably because, in bilayers, this motif best satisfies the predilection of the tryptophan residues to be disposed in the region of the membrane where the phospholipid headgroups and the electrolyte interpenetrate each other (reviewed for membrane proteins in general in Reithmeier, 1995, and for gramicidins in Koeppe and Andersen, 1996. A contrary view has been put forth by Burkhart et al., 1998, but the consensus of gramicidin workers still favors the single-helical motif as the dominant one in membranes).

The relatively small size of the gramicidin channel makes it an excellent model system on which to do molecular dynamics (MD) simulations that complement the extensive experimental investigations. A review of MD computations on gramicidin is given by Roux and Karplus (1994).

In early computations in our lab the explicit lipid environment was not included in MD simulations of gramicidin, because it was too computationally demanding to do so. Instead, the environment was approximated by a soft restraint on the atoms in the gramicidin molecule (Chiu et al., 1991). Woolf and Roux (1996) have done simulations of lipid in gramicidin with an 8:1 molecular ratio of lipid to gramicidin. For excess lipid, continuum calculations on the effect of gramicidin on the lipid structure have been done utilizing liquid crystal theory (Huang, 1986; Helfrich and Jakobsson, 1990; Ring, 1996).

In this paper we present MD simulations of gramicidin in excess lipid. The maximum feasible lipid/protein ratio was chosen to best emulate the "excess lipid" condition. The essential limitation was the size of the membrane patch that

Received for publication 5 February 1998 and in final form 19 January 1999.

Address reprint requests to Dr. Eric Jakobsson, Dept. of Biophysics, University of Illinois, 405 North Matthews Ave., 4309 Beckman Institute, Urbana, IL 61801. Tel.: 217-244-2896; Fax: 217-244-2909; E-mail: jake@ncsa.uiuc.edu.

0006-3495/99/04/1929/10 $2.00

could be computed in a reasonable time. These results are interpreted in the context of our previous simulations, the Woolf-Roux simulations, the liquid crystal calculations and related experiments, and experimental NMR measurements on the effect of gramicidin on lipid structure at various concentration (Rice and Oldfield, 1979). The Rice and Oldfield study is part of an extensive early literature on the effects of proteins on the structure and dynamics of "boundary lipids" (lipid molecules that are adjacent to proteins), that is well reviewed in Gennis, 1989, pp. 191–195.

METHODS

The overall strategy for computing the membrane preparation with incorporation of surface tension is similar to that presented in Chiu et al. (1995). Differences are stated below. In all other respects it can be assumed that the computations in this paper are methodologically the same as Chiu et al. (1995).

True constant surface tension (as opposed to constant lateral pressure) was used. The surface tension for the bilayer was set at 46 dyn/cm, based on the work of MacDonald and Simon (1987).

It should be noted that there is a current controversy among computational physical biochemists over whether or not the surface tension of a bilayer is nonzero (Jähnig, 1996; Feller and Pastor, 1996). The thermodynamics of the issue were discussed earlier by Tanford (1979) and White (1980). While of significant interest theoretically, the difference in computed properties between a bilayer at zero surface tension or the 46 dyn/cm we use may not be very great (Tieleman and Berendsen, 1996).

Following our previous published computation (Chiu et al., 1995) with a hydration level of 23 waters/lipid molecule, we computed a DMPC bilayer with 100 phospholipid molecules and 32 waters/lipid molecule and 46 dyn/cm surface tension (Chiu et al., 1996). The surface area per lipid molecule equilibrated to 61 $Å^2$ per phospholipid molecule. In our previously published work (Chiu et al., 1995) the surface areas was significantly lower, 57 $Å^2$/lipid. Aside from the above-mentioned modification in the boundary conditions (true constant surface tension as opposed to constant lateral pressure) the only difference between the two calculations was the amount of water, 23 waters/lipid in the first calculation and 36 waters/lipid in the second calculation (Chiu et al., 1996). We attribute most of the difference in the computed surface area to the difference in the amount of water in each simulation. At the end of a 770 ps simulation we removed two phospholipid molecules from each monolayer near the center of the simulated patch and inserted a gramicidin A channel containing nine water molecules in its lumen. The coordinates for the channel were kindly supplied Drs. Roger Koeppe and Tim Cross, as determined by NMR in their labs (Ketchem et al., 1993, 1997; Koeppe et al., 1994). Our dimer was assembled with one monomer in the configuration as determined by the Cross lab and the other in the configuration as determined by the Koeppe lab. The two configurations, both right-handed β-helices, are generally similar. The only tryptophan for which there is a significant difference in the initial side-chain conformation is #9. [Note that the assignment of conformations from the NMR results is not completely unambiguous (Koeppe et al., 1994).]

The complete computed system consisted of a GA channel, 96 DMPC molecules, and 3209 water molecules. It was energy minimized and then thermalized at 305 K with velocity reassignments for every 0.2 ps (100 time steps) for 50 ps. At this stage, position restraints to all GA atoms were applied with a harmonic force constant of 5000 kJ mol^{-1} $Å^{-2}$. In a subsequent MD run of 100 ps the restraining force was reduced to zero in 20 incremental step reductions of 250 kJ mol^{-1} $Å^{-2}$, with the reductions done at 5-ps intervals. The system was again thermalized at 305 K with velocity reassignments for 10 ps, and then subjected to continuous MD simulations. After 200 ps of continuous MD the system potential energy leveled off. Data collection began at this point. The data were saved at 50 fs (25 time step) intervals. Most of the simulations were done running 4-way parallel on the NCSA SGI Power Challenge Array. The computer time required was ~2 h/ps of simulated time when the computation was done in scalar mode on a single processor of the array. The calculation speeded up by a factor of 3.2 when done in 4-way parallel mode. The major obstacle to parallelizing more efficiently so that a larger number of processors could be efficiently employed is the serial nature of the SHAKE subroutine for re-setting the bond lengths. A snapshot of the fluid membrane with the inserted gramicidin and associated water is shown in Fig. 1.

RESULTS

Because of the propensity of Trp's to reside in the interfacial region of membrane proteins, it is of special interest to explore the interactions between Trp's and surroundings. In Fig. 2 we show the hydrogen bonding between Trp amide H's and surroundings. The Trp's 9, 11, 13, and 15 are in the monomer with initial conformation in the configuration as determined by the Cross lab, with the #15 Trp being closest to the bulk electrolyte. The Trp's 9′, 11′, 13′, and 15′ are in the monomer with initial conformation in the configuration as determined by the Koeppe lab, with the #15′ Trp being closest to the bulk electrolyte. The only major difference in the starting configuration for the aromatic residues between the two monomers is in the chi-1's and chi-2's of Trp's 9 and 9′. Fig. 2 *A* shows hydrogen bonds between the Trp's and water molecules; Fig. 2 *B* shows hydrogen bonds directly between the Trp's and the phospholipid molecules. The graphs show the time during which hydrogen bonds are formed; gaps in the horizontal lines represent intervals in which the hydrogen bonds are absent. (Note that because of the size of the symbols in the graph, very brief interruptions of hydrogen bonding will not be clearly visible.) Two patterns emerge: 1) all of the Trp's are hydrogen-bonded to the interfacial environment a large fraction of the time; and 2) there is much more hydrogen bonding with water than with phospholipid oxygens. The single exception to this last statement is the Trp 13′, which formed a long-lasting hydrogen bonding pattern to a phospholipid oxygen. We found that the nature of this long-lasting hydrogen bond was different from most of the Trp-lipid hydrogen bonds. By far the most common Trp-lipid hydrogen bond is with one of the carbonyl oxygens. A close look at the structure of the long-lasting hydrogen bonding pattern for Trp 13′ is shown in Fig. 2, *C–E*. It was seen that in this case the polar hydrogen in the Trp has formed a hydrogen bonding network with the O's in the glycerol moiety of the phospholipid molecule. Fig. 2, *C–E* are each snapshots chosen to represent the three configurations of the hydrogen network. Fig. 2 *C* shows an instantaneous configuration in which Trp-13′ is hydrogen bonded to the glycerol oxygen at the head of the Sn-1 chain. Fig. 2 *D* shows an instantaneous configuration in which Trp-13′ is hydrogen-bonded to the glycerol oxygen at the head of the Sn-2 chain. Fig. 2 *E* shows an instantaneous configuration in which Trp-13′ is simultaneously hydrogen-bonded to both glycerol oxygens. In the course of the simulation, the Trp-13′ NH shifts its hydrogen bond among the three configurations of Fig. 2,

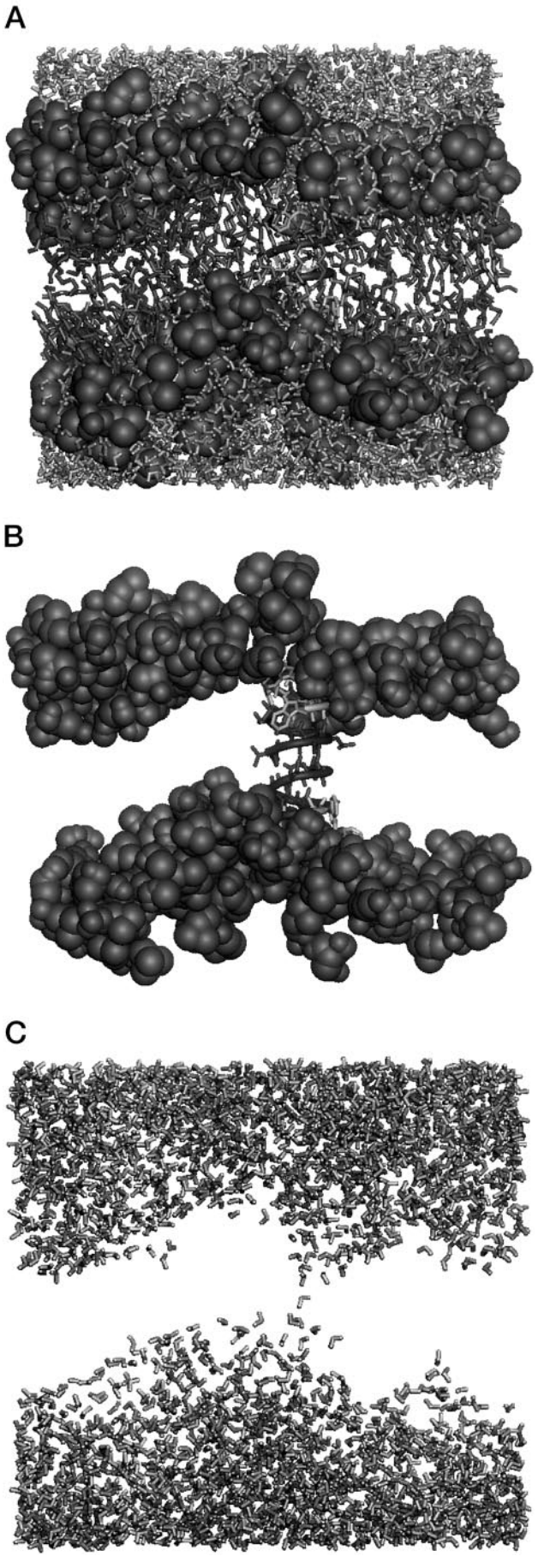

C–E, remaining in a local "cage" structure with both of them, as shown. This is an unusual but long-lasting configuration.

Fig. 3 shows the distributions of the side-chain torsion angles for all eight tryptophans in the channel. All of the distributions remained approximately centered about the initial NMR-derived configuration. None of the tryptophans made a distinct rotameric transition from the initial state to another state. For a couple of the Trp's, one can see significant but temporary excursion toward a second configuration, but no assumption of a second distinct rotameric state. Thus it seems that, although the two monomers had the side chains arranged in somewhat different configurations, both structures were sufficiently favorable energetically to retain their configurations throughout the course of the simulation.

In general, the side chains of the Val and Leu values in the computations explore a variety of configurations. The most frequent transitions are for the chi-2′ values of the Leu's, the least frequent transitions are for the Val's. In some cases, it does not seem that there is a clearly favored single side-chain conformation. There is no clear pattern between the two monomers as to which ones are more variable. In comparison to an early study on gramicidin in the absence of surrounding lipid (Chiu et al., 1992), it appears that the frequency of side-chain conformational transitions is about as high in the lipid as it is in vacuum.

Fig. 4 shows the backbone configurations of the channel. Fig. 4 *A* shows the computed mean value and rms deviation (*symbol with error bar*) of the phi angle compared with the initial configuration (*solid line*), for each of the residues in the two monomers. Fig. 4 *B* is in the same format as 4 *A*, but is for the psi angles. It is seen that the computed mean backbone configurations are similar to the initial NMR-derived configurations. Fig. 4 *C* shows the rms deviations in a separate plot. It can be seen that there are a couple of locations in which the channel backbone has exceptionally large flexure, at the center of the channel and at the mouth. In comparing this with an earlier study of the channel without a surrounding membrane (Chiu et al., 1991), it is seen that the rms deviations of the backbone are significantly larger, especially in the channel middle and at the mouths, in the membrane than in the earlier study. The earlier study used soft artificial restraints to maintain the secondary structure. It appears that even the softest artificial restraints we used inhibited the backbone flexure more than the membrane. However, the channel structure was completely stable in the membrane with no artificial restraints, whereas some artificial restraints were necessary in the earlier simulations to preserve the channel secondary structure.

FIGURE 1 Snapshot of the central computational cell of the computed preparation. (*A*) The entire preparation, water, gramicidin, and lipid. (*B*) The gramicidin and phospholipid headgroups only, showing the disposition of tryptophan residues in the headgroup region characteristic of membrane proteins. (*C*) Water only, displaying the penetration of water to the headgroup-hydrocarbon boundary characteristic of hydrated phospholipid membranes, and the chain of water through the gramicidin channel.

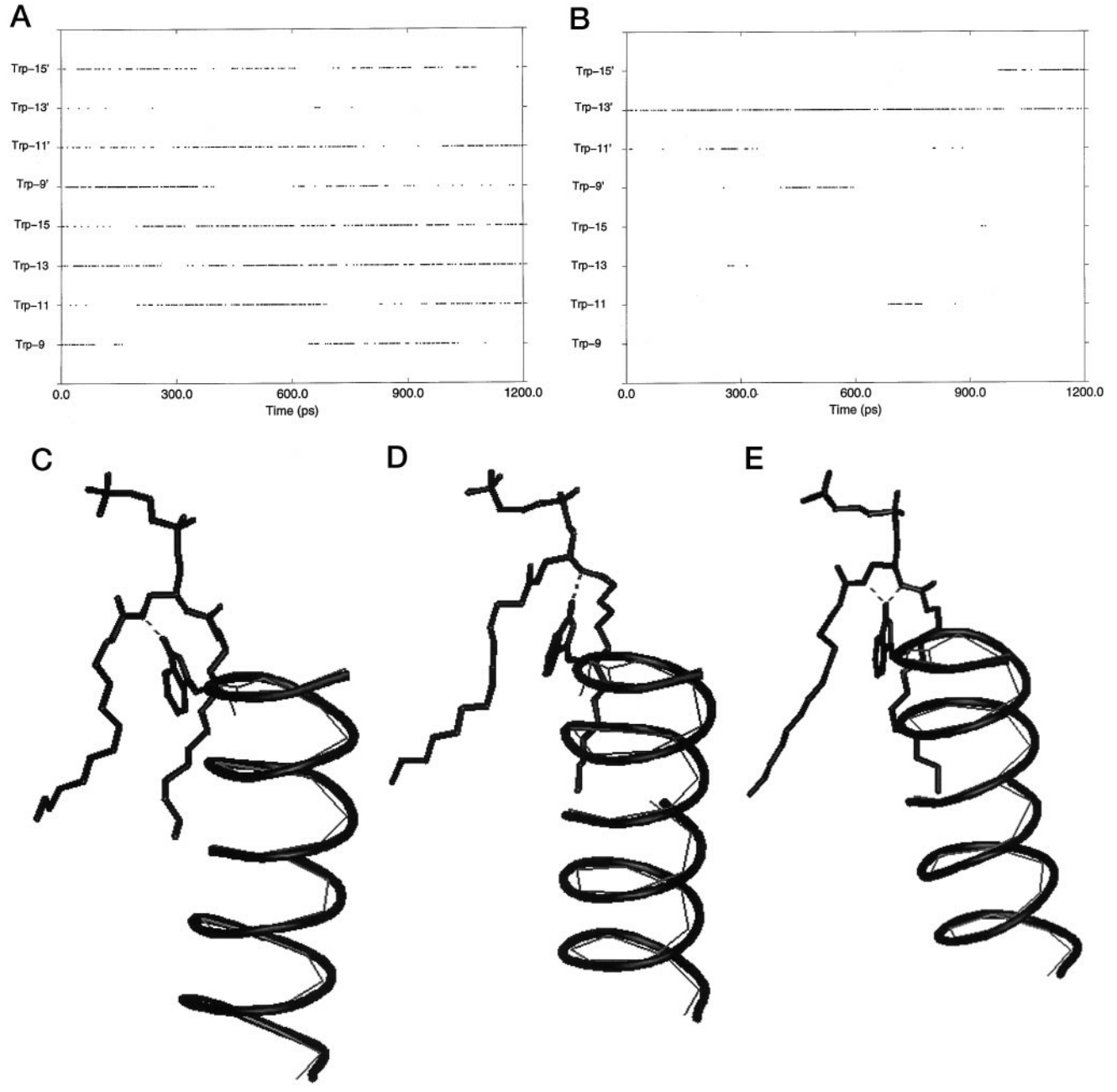

FIGURE 2 Hydrogen bonding of the Trp's. Numbers 9, 11, 13, and 15 are in one monomer of the channel, 9′, 11′, 13′, and 15′ are in the other monomer. (*A*) Time series for the hydrogen bonding of the Trp's to water in the interfacial region. (*B*) Time series for the hydrogen bonding of Trp's to phospholipid molecules. From (*A*) and (*B*) it can be seen that there is much more Trp hydrogen bonding for Trp's closer to the electrolyte (higher numbered residues) than for those closer to the hydrocarbon region, and that there is much more hydrogen bonding to waters than to phospholipid molecules (with the exception of 13′). (*C–E*) Conformation that resulted in a long-lived hydrogen bonding between Trp-13′ and one of the phospholipid molecules, in which the NH group on the Trp ring remained in close proximity to two oxygens from the glycerol group of one of the phospholipid molecules. (*C*) Snapshot showing the Trp-13′ NH hydrogen bonded to the glycerol oxygen at the head of the Sn-1 chain; (*D*) snapshot showing the Trp-13′ NH hydrogen bonded to the glycerol oxygen at the head of the Sn-2 chain; (*E*) snapshot showing the Trp-13′ NH simultaneously hydrogen-bonded to the glycerol oxygen at the head of both the Sn-1 and the Sn-2 chain.

Fig. 5 shows the order parameters for three classes of hydrocarbon chains: 1) the hydrocarbon chains in the lipid bilayer before the gramicidin was inserted (time-averaged for the 200 ps before insertion); 2) the hydrocarbon chains of lipids that were hydrogen-bonded to the gramicidin channel, either directly or via one intervening water, for at least 10% of the duration of the simulation; and 3) the hydrocarbon chains present during the gramicidin/lipid simulation that did not have close hydrogen bonding to the channel. It is seen that interaction with the gramicidin channel has the effect of significantly increasing the order of the lipids adjacent to the channel, but the presence of the channel does

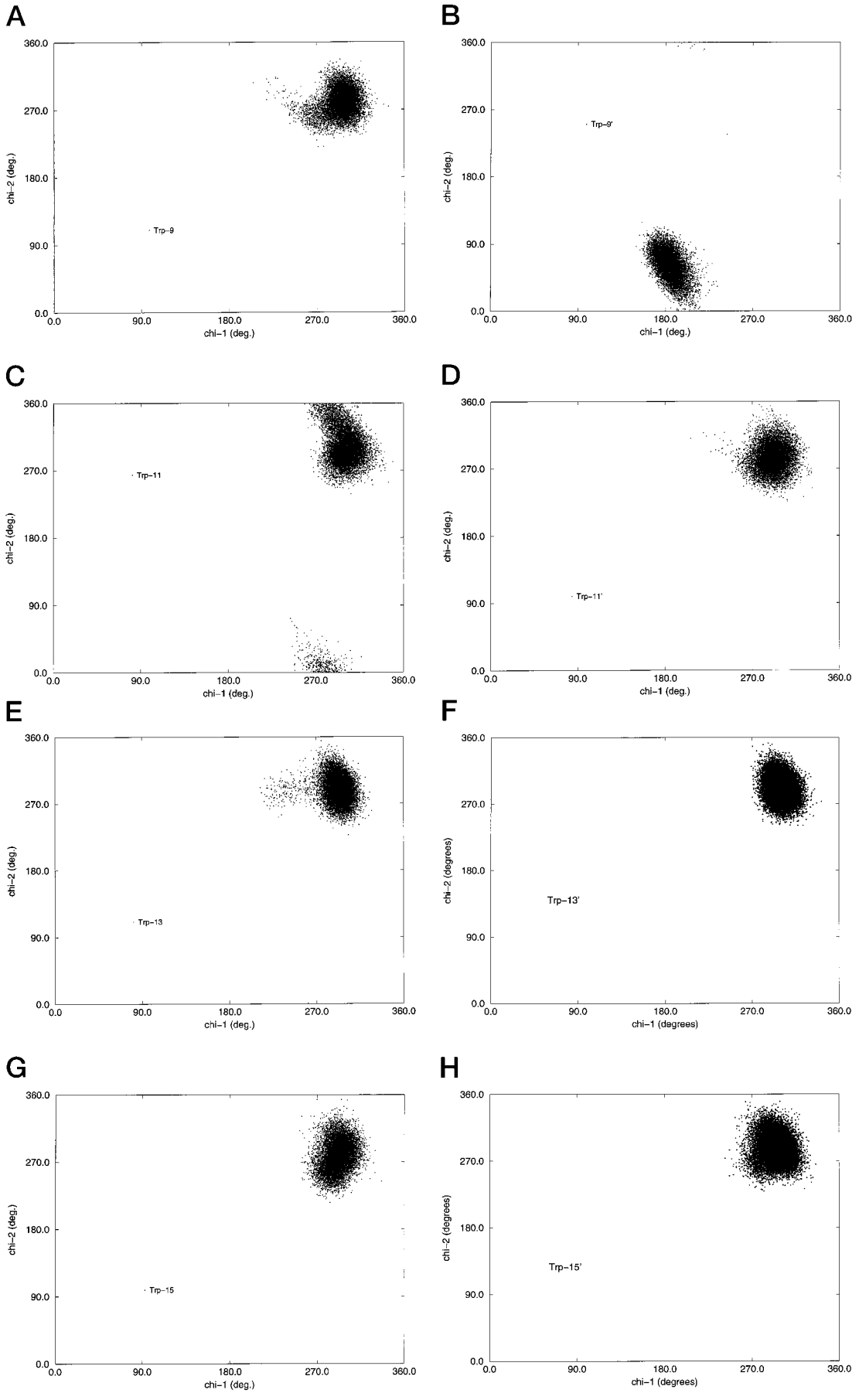
A
B
C
D
E
F
G
H
chi-2 (deg.)
chi-1 (deg.)
chi-2 (degrees)
chi-1 (degrees)
0.0
90.0
180.0
270.0
360.0
Trp-9
Trp-9'
Trp-11
Trp-11'
Trp-13
Trp-13'
Trp-15
Trp-15'

not have a significant effect on the ordering of the lipids that are not adjacent to the channel.

Table 1 shows the analysis of various structural features of the same three classes of lipids as are identified in Fig. 5. It is seen that the bilayer structure in general gets wider (the two interfacial regions get farther apart from each other) at the boundary with the gramicidin channel. This is seen in the increase in the carbonyl-carbonyl distance and the P-P distance. The widening of the membrane by these measures is consistent with the increase in the order parameters for these lipids shown in Fig. 5. The headgroup tilting is not quite as pronounced in the boundary lipids as the others, as shown by the fact that the N-P distance projected along the membrane normal direction goes from 1.0 Å in the lipids away from the membrane to 1.6 Å in the boundary lipids. However, even for the boundary lipids, the headgroup orientations, as determined by the direction of the N-P vector, are still more parallel than normal to the membrane plane. The other main point made by Fig. 5 and Table 1 is that the structure of the lipid away from the boundary in the gramicidin/lipid preparation is very similar to the lipid structure computed with no channel in the membrane at all.

DISCUSSION AND SUMMARY

This study is complementary to the studies of gramicidin in lipid from Woolf and Roux (1996). In those studies the gramicidin/lipid ratio was 1:8, representing a preparation dense in protein and well-aligned, ideal for solid-state NMR structural studies (Ketchem et al., 1993; Koeppe et al., 1994). Our preparation had excess lipid over protein, more typical for electrophysiological or water transport studies (Finkelstein, 1987).

With respect to protein-lipid interactions, our results show that the dominant hydrogen bonding of the tryptophan side chains is to water in the interfacial region. There is also hydrogen bonding directly between tryptophans and phospholipid molecules, but this is not as common as between tryptophans and water. In this respect our results are similar to those of Woolf and Roux (1996).

In a previous study (Chiu et al., 1992), we examined the side-chain conformations and frequency of conformational side-chain transitions in a simulated gramicidin channel with no surrounding lipid and no artificial restraints on the side-chain atoms. In that simulation the tryptophan side-chain dihedrals underwent far fewer rotameric transitions than the other side chains, but still averaged over one transition per angle per nanosecond (Chiu et al., 1992). Leucine and valine side chains underwent many side-chain transitions, especially Leu-4 and chi-2 of the other leucines. In the presence of the explicit lipid of the present simulation, the tryptophans were motionally restricted by the membrane, making no side-chain transitions at all. This is consistent with physical measurements that suggest that the tryptophans in this preparation are in a highly motionally restricted environment (Mukherjee and Chattopadhyay, 1994; Hu et al., 1995). Perhaps a major factor in the restriction is the ability of the indole NH to hydrogen-bond with its environment, either water or phospholipid. The valine and leucine side chains in the present study made transitions at a similar frequency to our previous vacuum study, so there was no evidence that the lipid in our preparation imposed serious motional restrictions on these side chains. This is in contrast to NMR studies suggesting much less motional freedom for the aliphatic side chain rotations than in our simulation (Lee and Cross, 1994; Lee et al., 1995; Ketchem et al., 1996). There are some possible reasons for the difference. One is that the experiments were done in an 8:1 lipid/gramicidin ratio and with incomplete hydration, rather than the excess lipid and water of our simulation. It may be that the lipid packs more closely around the gramicidin in that experimental situation than it does in excess lipid. It may also be that our computational technique for inserting the gramicidin and equilibrating it to the lipid did not result in sufficiently close packing to emulate the experiments in this regard. A "smart" Monte Carlo method such as Configuration Bias Monte Carlo (Scott, 1996) may be useful in finding more efficient packing between different molecular species in a heterogenous membrane, an approach that will be used in future work.

One tryptophan, 13′, exhibited persistent hydrogen bonding directly between the tryptophan residue and one of the phospholipid molecules. This was the only instance of a persistent hydrogen bonding between a tryptophan and a phospholipid. This hydrogen bonding was also unusual in that it was not with carbonyl oxygens but with oxygens of the glycerol group in the phospholipid. This tryptophan and the phospholipid got into a relative configuration in which the amide hydrogen was simultaneously quite close to two glycerol oxygens, and remained there throughout the simulation. It is hard to assess the significance of a singular event that occurs in an MD simulation, because one has no idea of the frequency of the event in longer time scales. With this caveat, we note that Mukherjee and Chattopadhyay (1994) proposed, based on fluorescence spectroscopy, that tryptophans in gramicidin could be divided into two classes with different local solvation environments. In their interpretation, one class consisted of Trp's 9 and 15, which are in a

FIGURE 3 Tryptophan side-chain conformers sampled during the simulation. Each dot on the graph is a conformer defined by chi-1 and chi-2. The conformation was sampled every picosecond, so each graph shows 1200 conformations. The natural minima, based on the symmetry of the bonds, are at 60, 180, and 300° for chi-1 and at 90 and 270° for chi-2. (*A*) Trp 9, initial configuration was chi-1 = 282°, chi-2 = 283°; (*B*) Trp 9′, initial configuration was chi-1 = 179°, chi-2 = 81°; (*C*) Trp 11, initial configuration was chi-1 = 288°, chi-2 = 297°; (*D*) Trp 11′, initial configuration was chi-1 = 293°, chi-2 = 297°; (*E*) Trp 13, initial configuration was chi-1 = 293°, chi-2 = 275°; (*F*) Trp 13′, initial configuration was chi-1 = 292°, chi-2 = 276°; (*G*) Trp 15, initial configuration was chi-1 = 299°, chi-2 = 259°; (*H*) Trp 15′, initial configuration was chi-1 = 290°, chi-2 = 274°.

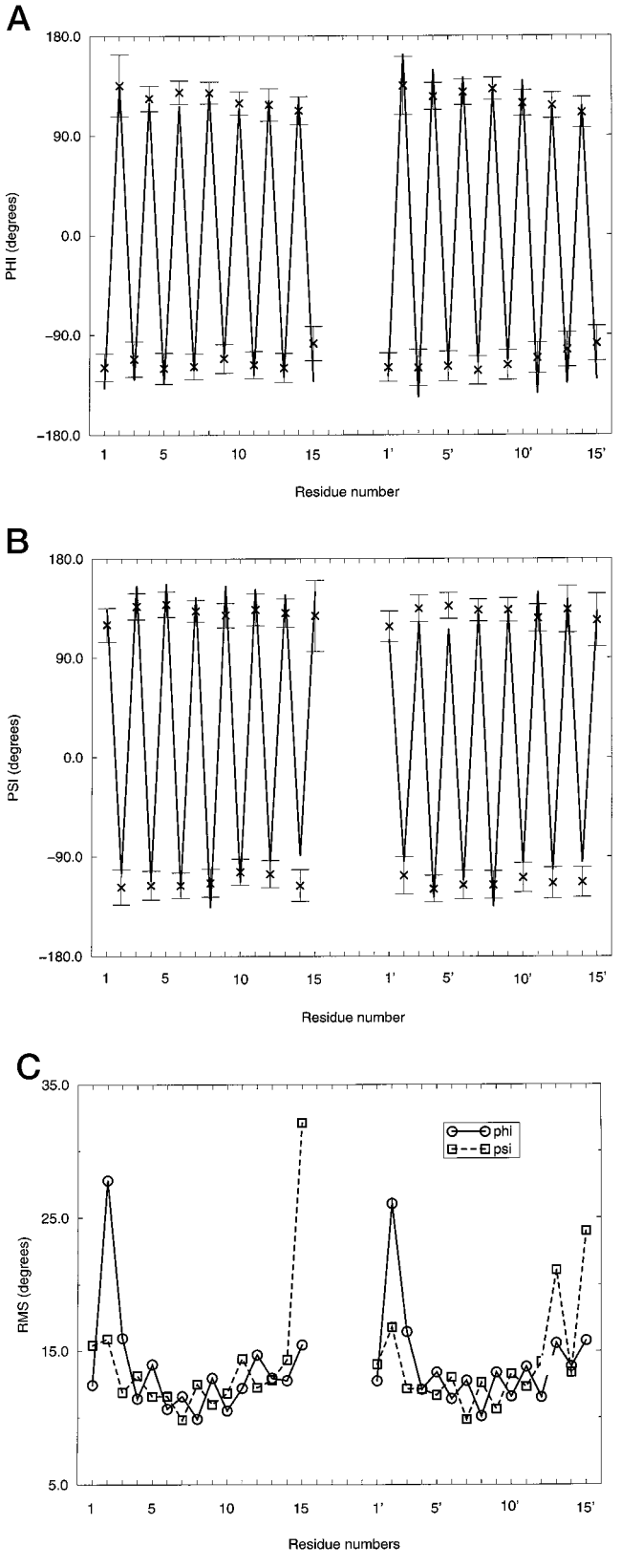

FIGURE 4 Backbone configurations of the channel. (*A*) Computed mean value and rms deviation (*symbol and error bar*) for the phi angle, as compared to the NMR-determined structure (*vertices of intersection of the solid line*), for each residue in the two monomers. (*B*) Same format as (*A*), for the psi angles. (*C*) Separate plot for the rms deviations, with circles representing the phi angles, and squares the psi angles.

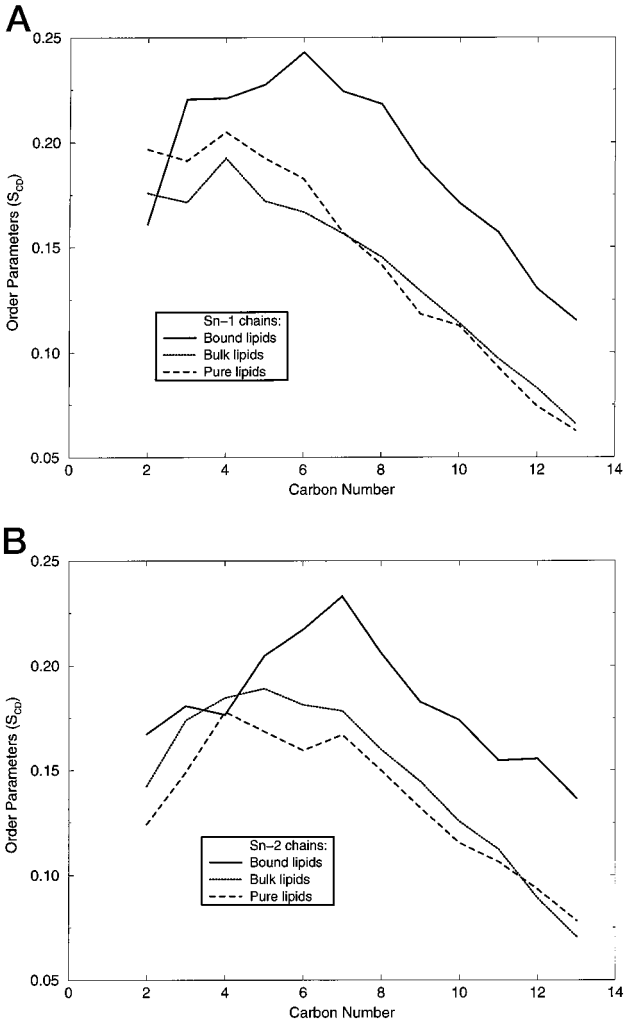

FIGURE 5 Hydrocarbon-chain order parameter profiles, for lipids with direct or indirect hydrogen bonding to the channel protein, for other lipids in the gramicidin/lipid preparation, and for the fluid lipid bilayer before insertion of the gramicidin. The criterion for direct or indirect hydrogen bonding to the protein is that the lipid must either be hydrogen-bonded directly to the protein, or must be hydrogen-bonded to a water molecule that is hydrogen-bonded to the protein, for at least 10% of the simulation time. (*A*) Order parameter profile for the Sn-1 chain, (*B*) order parameter profile for the Sn-2 chain.

position to stack with each other, while the other consists of Trp's 11 and 13, which are not in a potentially stacking orientation relative to each other. Our results suggest the possibility of an alternative interpretation that one of the classes consists of Trp's that make an almost continuous hydrogen bond with a phospholipid molecule for a long time.

It is difficult to draw any firm inferences about correlations between conformational changes of Trp side chains and alternative hydrogen bonding to adjacent water and lipid groups from our results. As mentioned above, it is clear from the fact that the Trp's made no large conformational changes that they are significantly motionally restricted by the water/lipid environment, but there is no obvious correlation between the amplitude of motions un-

TABLE 1 Structural features of the lipid membrane before and after gramicidin insertion

Structural Feature	Membrane Before Gramicidin Insertion	Gramicidin Neighbors	Non-neighboring Lipids After Gramicidin Insertion
Trans-gauche ratio, Sn-1 chain	3.02	3.76	2.89
Trans-gauche ratio, Sn-2 chain	2.82	2.97	2.80
N-N (choline) distance across bilayer (Å)	35.4, 0.3 rmsd	38.8, 0.6 rmsd	35.8, 0.4 rmsd
P-P distance across bilayer (Å)	33.6, 0.3 rmsd	36.0, 0.7 rmsd	34.2, 0.3 rmsd
N-P distance normal to membrane (Å)	0.9, 0.2 rmsd	1.6, 0.6 rmsd	0.8, 0.1 rmsd
Carbonyl-carbonyl distance across bilayer (Å)	25.7, 0.3 rmsd	28.3, 0.5 rmsd	26.2, 0.5 rmsd

In both cases the analyzed data are the last 500 ps of the simulation run. The data points for the distances are a time series with intervals of 50 fs, with the distances averaged across the entire preparation at each snapshot, resulting in the indicated mean values and root-mean-squared deviations. Note that the non-neighboring lipid membrane structure in the presence of gramicidin is similar to the membrane prior to gramicidin insertion. The membrane immediately adjacent to the gramicidin is wider than the rest of the membrane and structurally similar to the first lipid layer in a preparation with only eight lipids per gramicidin molecule (Woolf and Roux, 1996).

dergone by individual Trp's and the specific hydrogen-bonding environments of those particular Trp's. For example, it is clear from Fig. 2 that Trp 9′ is hydrogen-bonded to either a water or a lipid molecule a much larger fraction of the time than its counterpart Trp 9 in the other monomer of the channel. Yet from Fig. 3 it does not seem that there is any marked difference between Trp 9 and Trp 9′ in the magnitude of the conformational fluctuations they undergo. Trp 13 appears to undergo some larger excursions than does Trp 13′ (the Trp that anomalously hydrogen-bonded directly to one of the lipid molecules), but other Trp's that did not extensively hydrogen-bond directly to lipid molecules had conformational fluctuations that were as limited as Trp13′. It appears that the conformational sampling available from a 1-ns MD simulation is not sufficient to determine the correlation between specific Trp/lipid/water hydrogen bonding relationships and conformational changes of Trp side chains.

Insertion of the gramicidin channel caused an increase in the order parameters of the hydrocarbon chains of those phospholipids adjacent to the gramicidin channel, as seen in Fig. 4. The order parameters of the other lipid molecule chains seemed not to be greatly affected. The order parameters are not quite as large as in computed (Woolf and Roux, 1996) or experimental (Rice and Oldfield, 1979) systems in which the lipid/gramicidin ratio is much lower than in our simulations. However, the pattern of our observed order parameter profile is similar to those results, in that there is a distinct peak in the region of the hydrocarbon chain nearer to the interfacial region. Thus our results suggest that the gramicidin channel has the effect of increasing the order parameter of DMPC hydrocarbon chains adjacent to it, in the excess lipid of our simulation as well as in preparations in which there is only an effective single shell of lipids around the channel (Rice and Oldfield, 1979; Woolf and Roux, 1996). Monte Carlo calculations of a 14-carbon saturated hydrocarbon chain adjacent to a gramicidin channel also show an increase in the order parameter for the positions in the chain nearer the interfacial region, relative to the order parameters for lipid in the absence of the channel (Xing and Scott, 1992).

Table 1 shows that the membrane adjacent to the channel is thicker than the rest of the membrane. Our gramicidin-neighboring lipids are similar in respect to thickness to the lipids in the Woolf and Roux (1996) study. As measured by the mean carbonyl-carbonyl distance, the hydrophobic thickness of the membrane adjacent to the channel is 28.3 Å, in contrast to 26.2 Å in the rest of the membrane. Our results and those of Woolf and Roux are also consistent with NMR studies showing, over a wide range of concentrations, that the presence of gramicidin increases the order parameter of DMPC membranes (Rice and Oldfield, 1979). The most straightforward inference that arises from comparing the Woolf-Roux results to ours is that the structure of the nearest-neighbor lipids to the gramicidin is dominated by the local interactions between the neighbor lipids and the gramicidin, and not as much influenced by the other lipids. Based on the similarity of our bulk lipid results to the non-neighbor lipids in the gramicidin/lipid calculation, it appears that the presence of the gramicidin does not influence the lipid structures very much past the nearest neighbors, at least in DMPC.

However, the above interpretation is in apparent contradiction to the assumptions of several previous studies in which the conformation around the gramicidin channel was calculated from liquid crystal theory (Helfrich and Jakobsson, 1990; Huang, 1986; Ring, 1996). In the Huang and Helfrich/Jakobsson studies it was assumed that the gramicidin channel would cause a thinning in its immediate vicinity of a phospholipid membrane as thick as DMPC. The experimental basis for this assumption was the finding that the mean gramicidin channel lifetime in monoacylglycerol-squalene bilayers is increased as the bilayer hydrophobic thickness is reduced to 21.7 Å, but not increased further for further reductions in hydrophobic thickness (Elliot et al., 1983). From this it was deduced that the gramicidin lipophilic region has a length of 21.7 Å, and the adjacent lipid thins down to match that. Ring (1996) has also used con-

tinuum theory in conjunction with the experimental results of Elliot et al. (1983) to consider the form of the lipid bilayer near the gramicidin channel. Based on the dependence of gramicidin lifetime on glycerol monooleate (GMO) membrane surface tension, Ring argued that the lipid bilayer thickness in the first layer of lipids nearest to the gramicidin would not thin down all the way to the hydrophobic thickness, but would be at some thickness intermediate between 21.7 Å and the unperturbed hydrophobic thickness of the membrane. The results in the present paper are totally different, as the hydrophobic thickness adjacent to the gramicidin *increased* over the unperturbed 25 Å hydrophobic thickness of the membrane.

Our results must also be considered in the context of the work of Goulian et al. (1998), who found that gramicidin channel formation rate and lifetime in DOPC vesicles increase with applied tension. Their interpretation is that the tension reduces the hydrophobic thickness of the membrane, thus providing a better match between the hydrophobic length of the channel and the hydrophobic thickness of the membrane. This interpretation is consistent with the previously published liquid crystal continuum calculations on the membrane deformation around the channel, but does not seem consistent with the MD results of the lipid conformation around the channel presented in this paper. The sum total of the above results poses a quandary for interpretation. From the MD simulations and the NMR order parameter results, it is logical to infer that the membrane is thicker adjacent to the gramicidin channel than if the inference is made from channel rate-of-formation and lifetime results combined with a liquid crystal description of the membrane. We will suggest an interpretation below to resolve these apparent contradictions.

It may be that one difference between these conclusions from the MD results and the assumptions underlying the liquid crystal calculations (Huang, 1986; Helfrich and Jakobsson, 1990; Ring, 1996) is that those assumptions were based on experiments in GMO membranes. Since the GMO studies and the first liquid crystal calculations, much information has emerged on the special role of aromatic side chains, especially tryptophans, in "anchoring" membrane proteins in the interfacial region of biological membranes. This information comes from the observed distribution of tryptophan residues in naturally occurring membrane proteins (Reithmeier, 1995), from mutations of tryptophan residues in gramicidin (Koeppe and Andersen, 1996), and from free energy measurements of partitioning of aromatic residues in the interfacial region of phospholipid membranes (Wimley and White, 1996). We note that the interfacial region will have significantly different character in phospholipid and in glycerol membranes. It may be that, as a consequence of differences in the interfacial region, the effective lipophilic thickness of the gramicidin channel is longer in DMPC membranes than in the GMO membranes from which the previous inferences were drawn. Recent work (Lundbaek et al., 1997) has shown that modifying electrostatic interaction among phospholipid headgroups, by changing ionic concentrations, can modify the stability and lifetime of embedded gramicidin channels. Thus, comparing results of different experiments on lipid-gramicidin interactions, if the lipids are of different types, or if relevant experimental conditions are different, may lead to error.

However, one must deal with the results of Goulian et al. (1998), which were done in DOPC membranes. Here, an increased dimer formation when the membrane was put under tension was ascribed to improved hydrophobic matching when the tension thinned the membrane, counter to the above argument that the effective hydrophobic length of the channel may be longer in PC membranes than in glycerol membranes. In this case we suggest that an alternative process could lead to increased dimer formation as the membrane is put under tension, and that is increased lateral mobility of the monomers, as the membrane becomes thinner. By this interpretation, as the surface area per phospholipid increases under tension, the wider spacing between the phospholipid molecules results in an increased lateral diffusion coefficient for the gramicidin monomers, so the frequency with which they encounter each other in the docking position increases. In this view, although the channel formation frequency would increase with tension, the channel lifetime would not be significantly affected, which is consistent with the Goulian et al. data. This is in contrast to a study in which the channel formation rate was changed by the degree of phospholipid chain saturation, where the channel lifetime is substantially increased by the same change that increases rate of channel formation (Girshman et al., 1997).

Whatever the ultimately correct interpretations of the above and future results, it is remarkable that computations and experiments on such an irreducibly simple channel-membrane system (the simplest known ion channel in a lipid membrane of homogenous composition), a system that has been studied for decades, can still give rise to the need for such complex interpretations of the data to resolve all the observations.

The authors are grateful to Roger Koeppe and Tim Cross for providing NMR-derived coordinate files for the initial configurations of the gramicidin monomers.

This work was supported by a grant from the National Science Foundation. Computations were done on the Silicon Graphics Power Challenge Array at the National Center for Supercomputing Applications.

REFERENCES

Burkhart, B. M., N. Li, D. A. Langs, W. A. Pangborn, and W. L. Duax. 1998. The conducting form of gramicidin A is a right-handed double-stranded double helix. *PNAS.* 95:12950–12955.

Chiu, S.-W., M. Clark, V. Balaji, S. Subramaniam, H. L. Scott, and E. Jakobsson. 1995. Incorporation of surface tension into molecular dynamics simulation of an interface: A fluid phase lipid bilayer membrane. *Biophys. J.* 69:1230–1245.

Chiu, S. W., K. Gulukota, and E. Jakobsson. 1992. Computational approaches to understanding the ion channel-lipid system. *In* Membrane Proteins: Structures, Interactions, and Models. A. Pullman, B. Pullman, and J. Jortner, editors. Kluwer, The Netherlands.

Chiu, S.-W., E. Jakobsson, S. Subramaniam, and J. A. McCammon. 1991. Time-correlation analysis of simulated water motion in flexible and rigid gramicidin channels. *Biophys. J.* 60:273–285.

Chiu, S.-W., S. Subramaniam, and E. Jakobsson. 1996. Simulation of a fully hydrated DMPC bilayer using the NγT boundary conditions. *Biophys. J.* 70:94*a*. (Abstr.).

Dubos, R. J., and R. D. Hotchkiss. 1941. The production of bactericidal substances by aerobic sporulating bacilli. *J. Exp. Med.* 73:629–640.

Elliot, J. R., D. Needham, J. P. Dilger, and D. A. Haydon. 1983. The effect of bilayer thickness and tension on gramicidin single-channel lifetime. *Biochim. Biophys. Acta*. 735:95–103.

Feller, S. E., and R. W. Pastor. 1996. On simulating lipid bilayers with an applied surface tension: Periodic boundary conditions and undulations. *Biophys. J.* 71:1350–1355.

Finkelstein, A. 1987. Water Movement through Lipid Bilayers, Pores, and Plasma Membranes. Theory and Reality. Wiley-Interscience, New York.

Gennis, R. B. 1989. Biomembranes. Molecular Structure and Function. Springer-Verlag, New York.

Girshman, J., D. V. Greathouse, R. E. Koeppe, 2nd, and O. S. Andersen. 1997. Gramicidin channels in phospholipid bilayers with unsaturated acyl chains. *Biophys. J.* 73:1310–1319.

Goulian, M., O. N. Mesquita, D. K. Fygenson, C. Nielsen, O. S. Andersen, and A. Libchaber. 1998. Gramicidin channel kinetics under tension. *Biophys. J.* 74:328–337.

Helfrich, P., and E. Jakobsson. 1990. Calculation of deformation energies and conformations in lipid membranes containing gramicidin channels. *Biophys. J.* 57:1075–1084.

Hladky, S. B., and D. A. Haydon. 1970. Discreteness of conductance change in bimolecular lipid membranes in the presence of certain antibiotics. *Nature*. 225:451–453.

Hu, W., N. D. Lazo, and T. A. Cross. 1995. Tryptophan dynamics and structural refinement in a lipid bilayer environment: solid state NMR of the gramicidin channel. *Biochemistry*. 34:14138–14146.

Huang, H. W. 1986. Deformation free energy of bilayer membrane and its effect on gramicdiin channel lifetime. *Biophys. J.* 50:1061–1070.

Jähnig, F. 1996. What is the surface tension of a lipid bilayer membrane? *Biophys. J.* 71:1348–1349.

Ketchem, R. R., W. Hu, and T. A. Cross. 1993. High-resolution conformation of gramicidin A in a lipid bilayer by solid-state NMR. *Science*. 261:1457–1460.

Ketchem, R. R., K.-C. Lee, S. Huo, and T. A. Cross. 1996. Macromolecular structural elucidation with solid-state NMR-derived orientational constraints. *J. Biomol. NMR*. 8:1–14. mcKetchem, R. R., B. Roux, and T. A. Cross. 1997. High-resolution polypeptide structure in a lamellar phase lipid environment from solid state NMR derived orientational constraints. *Structure*. 5:1655–1669.

Koeppe, R. E. II, and O. S. Andersen. 1996. Engineering the gramicidin channel. *Annu. Rev. Biophys. Biomol. Struct.* 25:231–258.

Koeppe, R. E. II, J. A. Killian, and D. V. Greathouse. 1994. Orientations of the tryptophan 9 and 11 side chains of the gramicidin channel based on deuterium nuclear magnetic resonance spectroscopy. *Biophys. J.* 66:14–24.

Langs, D. A. 1988. Three-dimensional structure at 0.86 Å of the uncomplexed form of the transmembrane ion channel peptide gramicidin A. *Science*. 241:188–191.

Lee, K.-C., and T. A. Cross. 1994. Side-chain structure and dynamics at the lipid-protein interface: Val-1 of the gramicidin A channel. *Biophys. J.* 66:1380–1387.

Lee, K.-C., S. Huo, and T. A. Cross. 1995. Lipid-peptide interface: valine conformation and dynamics in the gramicidin channel. *Biochemistry*. 34:857–867.

Lundbaek, J. A., A. M. Maer, and O. S. Andersen. 1997. Lipid bilayer electrostatic energy, curvature stress, and assembly of gramicidin channels. *Biochemistry*. 36:5695–5701.

MacDonald, R. C., and S. A. Simon. 1987. Lipid monolayer states and their relation to bilayers. *Proc. Natl. Acad. Sci. USA*. 84:4089–4093.

Mukherjee, S., and A. Chattopadhyay. 1994. Motionally restricted tryptophan environments at the peptide-lipid interface of gramicidin channels. *Biochemistry*. 33:5089–5097.

Reithmeier, R. A. 1995. Characterization and modeling of membrane proteins using sequence analysis. *Curr. Opin. Struct. Biol.* 5:491–500.

Rice, D., and E. Oldfield. 1979. Deuterium nuclear magnetic resonance studies of the interaction between dimyristoylphosphatidylcholine and gramicidin A. *Biochemistry*. 18:3272–3279.

Ring, A. 1996. Gramicidin channel-induced lipid membrane deformation energy. Influence of chain length and boundary conditions. *Biochim. Biophys. Acta*. 1278:147–159.

Roux, B., and M. Karplus. 1994. Molecular dynamics simulations of the gramicidin channel. *Annu. Rev. Biophys. Biomol. Struct.* 23:731–761.

Scott, H. L. 1996. Statistical mechanics and Monte Carlo studies of lipid membranes. *In*Biological Membranes. A Molecular Perspective from Computation and Experiment. K. M. Merz and B. Roux, editors. Birkhäuser, Boston. 83–104.

Tanford, C. 1979. Hydrostatic pressure in small phospholipid vesicles. *Proc. Natl. Acad. Sci. USA*. 76:3318–3319.

Tieleman, D. P., and H. J. C. Berendsen. 1996. Molecular dynamics simulations of a fully hydrated dipalmitoyl phosphatidylcholine bilayer with different macroscopic boundary conditions and parameters. *J. Chem. Phys.* 105:4871–4880.

Urry, D. W. 1971. The gramicidin A transmembrane channel: a proposed π(L, D) helix. *Proc. Natl. Acad. Sci. USA*. 68:672–676.

Wallace, B. A., and K. Ravikumar. 1988. The gramicidin pore: crystal structure of a cesium complex. *Science*. 241:182–187.

White, S. H. 1980. Small phospholipid vesicles: internal pressure, surface tension, and surface free energy. *Proc. Natl. Acad. Sci. USA*. 77: 4048–4050.

Wimley, W. C., and S. H. White. 1996. Experimentally determined hydrophobicity scale for proteins at membrane interfaces. *Nature Struct. Biol.* 3:842–848.

Woolf, T. B., and B. Roux. 1996. Structure, energetics, and dynamics of lipid-protein interactions: a molecular dynamics study of the gramicidin A channel in a DMPC bilayer. *Proteins: Struct., Funct., Genet.* 24: 92–114.

Xing, J., and H. L. Scott. 1992. Monte Carlo studies of a model for lipid-gramicidin A bilayers. *Biochim. Biophys. Acta*. 1106:227–232.